CrossMark

ORIGINAL ARTICLE

Alunite characterization in the upper Eocene clay deposits of Central Tunisia: an implication to its genesis

Mohamed Essghaier Gaied · Fredj Chaabani · Wissem Gallala

Abstract Alunite mineral was recently identified at the upper Eocene clay deposits associated with laminated primary gypsum and iron oxide in Central Tunisia, particularly at El Gnater site. The alunite characterization has been performed by several analytical techniques [atomic absorption spectroscopy (AAS), X- ray diffraction (XRD), scanning electron microscope (SEM), thermogravimetric analysis (TGA) and differential thermal analysis (DTA)]. The mean features of their chemical composition are its deficiency of Al, water excess content, small replacement of K by Na and absence of impurities such as Fe. The X-ray diffraction pattern reveals the purity of the alunite samples. The SEM micromorphological study shows a compact facies which is made up by homogeneous pseudocubic microcrystals having approximately the same diameters of 1 μm. Thermal behaviour of El Gnater alunite closely matches published literature which shows two major endothermic peaks at 528 and 744 °C with total weight loss 17.27 and 29.09 %, respectively. The former corresponds to the dehydroxylation processes and the latter corresponds to sulphate decomposition reaction. The association of studied alunite with laminated primary gypsum, hematite and clay minerals implies its late diagenetic origin in reduced conditions and in evaporitic environment. However, jarosite was produced by oxidation of pyrite which was very abundant in the claystone host.

M. E. Gaied
Institute of Fine Arts, Place de la Gare, Sousse, Tunisia

F. Chaabani
Geology Department, Faculty of Sciences of Tunis,
L.R: Ressources Minérales, El Manar, Tunisia

W. Gallala (✉)
Faculty of Sciences of Gabes, Department of Earth Sciences,
Riadh City, Zirig, 6072 Gabès, Tunisia
e-mail: gallala_wissem@yahoo.fr

Introduction

In general, minerals of alunite group are generally described in the products of hydrothermal alteration of volcanic materials (Ross et al. 1968; Mutlu et al. 2005) and also in sedimentary deposits where they are often considered as weathering products of clays (Keller et al. 1967; Goldbery 1980; Chitale and Güven 1987; Rouchy and Pierre 1987; Khalaf 1990; Long et al. 1992). In both these cases, Al-minerals are alunitized by sulphuric acid, which is generated by the oxidation of hydrogen sulphide or of metallic sulphides during early or late stages of diagenesis (Lombardi and Sheppard 1977; Hall 1978; Goldbery 1980).

Alunite associated with halloysite has been reported in Lechuguilla cave in the Guadalupe Mountains and has been assumed to be an alteration product of the clay host, which is also due to the action of sulphuric acid (Palmer and Palmer 1992).

Occurrence of early diagenetic Na–alunite was recently described in the Middle Miocene evaporitic succession from the Sinai at Ras Sudar on the eastern coast of the Gulf of Suez.

Na–alunite was developed within cryptalgal sediments which end a regressive sedimentary sequence represented by intertidal lithofacies grading to subtidal lithofacies. Its formation was related to bacterial sulphate reduction, followed by the reoxidation of sulphide and production of sulphuric acid which reacted with clays (Goldbery 1980).
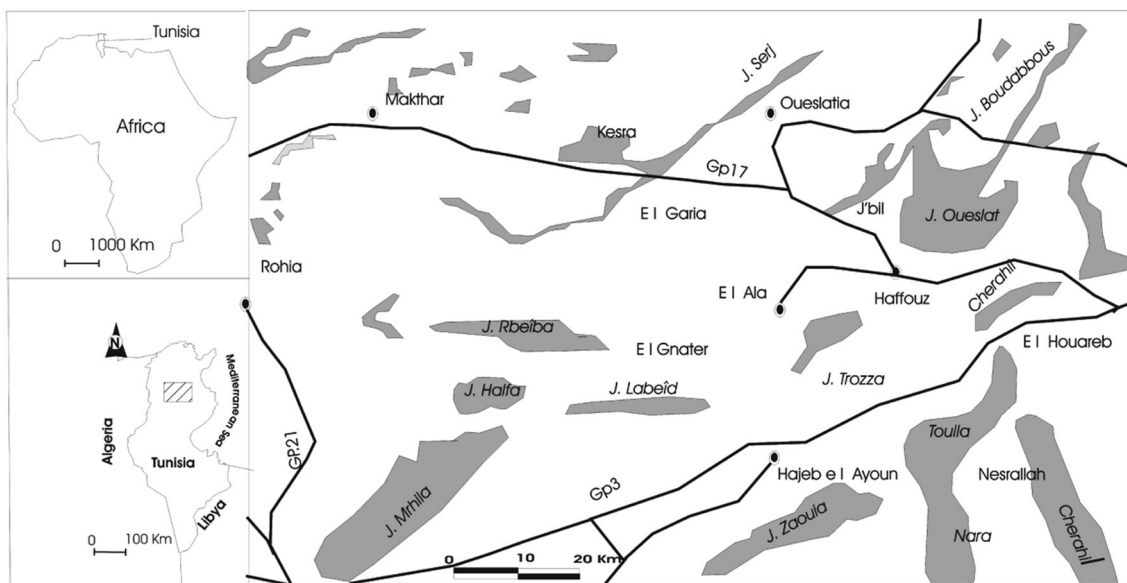
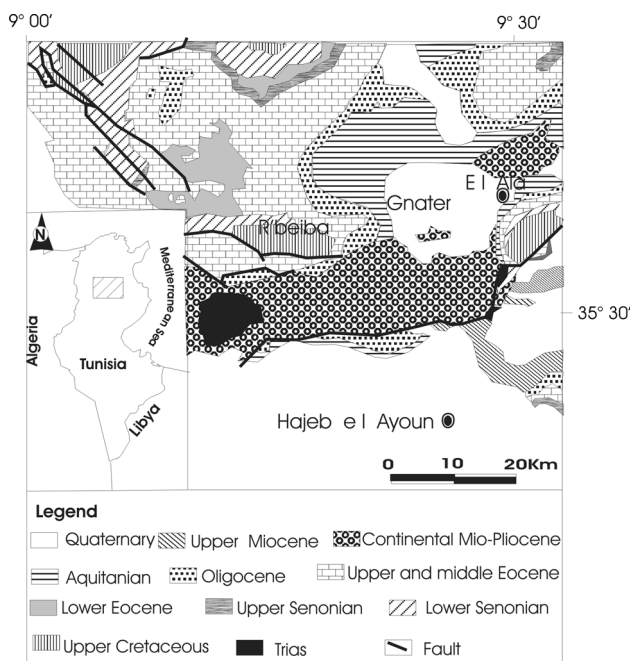**Fig. 1** Geographic location map of El Gnater region

Fig. 2 Geological location of El Gnater sector

Rouchy and Pierre (1987), presented a new finding of sedimentary natroalunite in the middle Miocene evaporated cap rock of the diapir on the Gemsa Peninsula, in the southwestern coast of the Gulf of Suez. In this case, sedimentological and isotopic data demonstrate the late diagenetic origin of Na–alunite.

Alunite–jarosite minerals can be described by the general structural formula $MR_3(SO_4)_2(OH)_6$; where M is the 12-fold coordination site, commonly occupied by large cations: K^+, Na^+, Rb^+, NH_4^+, Ag^+, H_3O^+, Ca^{2+}, Pb^{2+}, Ba^{t+}, Sr^{2+}, Ce^{3+}, Ti^+, Hg^{2+}; and R is the octahedral coordinated site which is occupied by Al^{3+} (for alunite) or Fe^{3+} (for jarosite); whereas the sulphate tetrahedral can be replaced by PO_4^{2-}, AsO_4^{2-} or CrO_4^{2-} (Ossaka et al. 1982; Hartig et al. 1984; Scott 1987, 2000; Long et al. 1992; Stoffregen and Alpers 1992; Rattray et al. 1996; Dutrizac and Jambor 2000; Stoffregen et al. 2000; Drouet and Navrotsky 2003; Rudolf et al. 2003; Drouet et al. 2004). For the alunite structure $MAl_3(SO_4)_2(OH)_6$, the most frequent chemical substitutions in M site, are K^+, Na^+, H_3O^+. This may reduce the extension of the natural solid solutions to the ternary system (K^+, Na^+, H_3O^+) for the triangle: alunite, natroalunite and hydronium alunite, as given by the following general formula $K_{1-X-y}Na_y(H_3O)_XAl_w(SO_4)_2(OH)_{6-3(3-z-w)}(H_2O)_{3(3-z-w)}$ proposed by Drouet et al. (2004), in which implies non-stoichiometry of alunite species and an excess of water due to the lack of Al (Hartig et al. 1984; Bohmhammel et al. 1987; Ripmeester et al. 1986; Lager et al. 2001).

Tunisian alunite has been twice reported, in El Gnater site, during a regional geological survey of the area by Gaied (1991, 1996), who gives some geological details about this recent discovered occurrence.

The main aim of this work is to give some further information about the geological setting as well as the mineralogical characterization of alunite at El Gnater site (Kairouan District) of Central Tunisia. This is to clarify the genesis of the studied alunite.
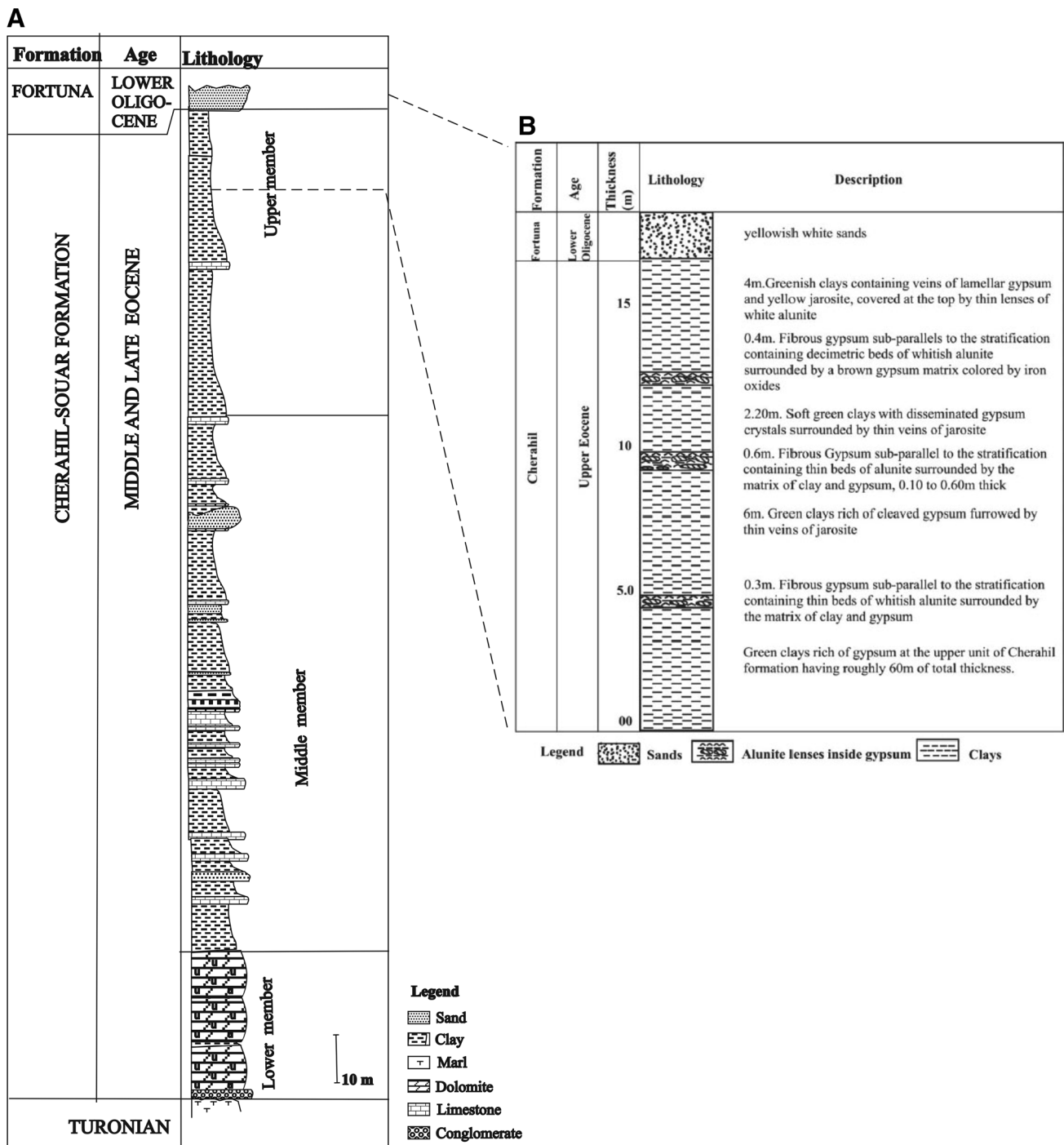
A

Formation	Age	Lithology
FORTUNA	LOWER OLIGO-CENE	
CHERAHIL-SOUAR FORMATION	MIDDLE AND LATE EOCENE	Upper member / Middle member / Lower member
	TURONIAN	

Legend
- Sand
- Clay
- Marl
- Dolomite
- Limestone
- Conglomerate

10 m

B

Formation	Age	Thickness (m)	Lithology	Description
Fortuna	Lower Oligocene			yellowish white sands
Cherahil	Upper Eocene	15		4m.Greenish clays containing veins of lamellar gypsum and yellow jarosite, covered at the top by thin lenses of white alunite
				0.4m. Fibrous gypsum sub-parallels to the stratification containing decimetric beds of whitish alunite surrounded by a brown gypsum matrix colored by iron oxides
		10		2.20m. Soft green clays with disseminated gypsum crystals surrounded by thin veins of jarosite
				0.6m. Fibrous Gypsum sub-parallel to the stratification containing thin beds of alunite surrounded by the matrix of clay and gypsum, 0.10 to 0.60m thick
				6m. Green clays rich of cleaved gypsum furrowed by thin veins of jarosite
		5.0		0.3m. Fibrous gypsum sub-parallel to the stratification containing thin beds of whitish alunite surrounded by the matrix of clay and gypsum
				Green clays rich of gypsum at the upper unit of Cherahil formation having roughly 60m of total thickness.
		00		

Legend: Sands — Alunite lenses inside gypsum — Clays

Fig. 3 **a** Lithological section of El Gnater sector; **b** details of the upper member of Cherahil formation showing lenticular alunite horizons

Analytical methods

In order to isolate any contamination, El Gnater alunite was sampled with a geologist hammer and carefully separated from its coat, which is made up by gypsum and hematite. Chemical analysis of two samples was carried out at the Tunisian National Institute of Scientific and Technological

Research "Institut National de Recherche Scientifique et Technologique (I.N.R.S.T.)" and at the National Mines Board "Office National des Mines (O.N.M)", with atomic absorption spectroscopy for K_2O, Na_2O, CaO, MgO, Fe_2O_3, Al_2O_3 and SiO_2. The gravimetric method is used only for SO_3.

The total water amount was determined by two different methods: from thermogravimetric curve and by heating the

Fig. 4 Mineralogical association of El Gnater deposits showing the upper level of white alunite nodules (**a**), Jarosite and lamellar gypsum (**b**), details of an alunite nodule that is surrounding by laminated primary gypsum and locally by iron oxide
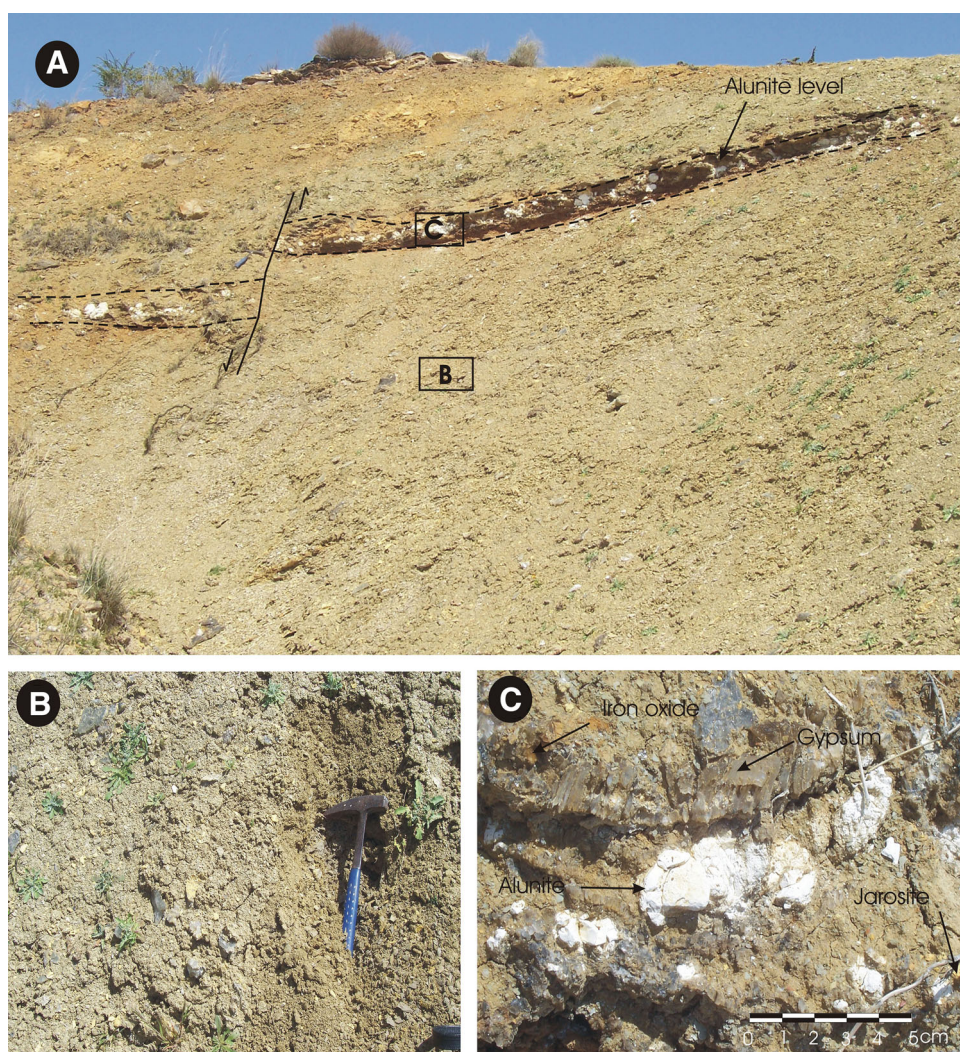

Table 1 Analysed chemical composition of alunites

	K_2O	Na_2O	CaO	Al_2O_3	SiO_2	MgO	Fe_2O_3	SO_3	LIO	Total
Alunite this work (1)	9.15	2.16	0.00	31.15	0.43	0.03	0.3	36.48	17.80	97.47
									17.27€	
Alunite ideal (2)	11.40	0	0	37.00	0	0	0	38.60	13.0	100
Natroalunite ideal (3)	0	7.8	0	38.4	0	0	0	40.20	13.6	100
H_3O–alunite ideal (4)	0	0	0	38.81	0	0	0	40.63	20.55	100
Alunite[a] (5)	10.0	NA	NA	32.3	NA	NA	NA	38.4	13.04	93.7
H_3O–alunite ideal[a] (6)	NA	0.1	0.5	36.5	NA	NA	NA	41.42	20.1	98.6

LIO loss on ignition by heating at 600 °C, € the water loss at 600 °C, calculated from DTA curve, *NA* non analysed

Chemical composition of natural alunite, this work, compared with three calculated ideal end members of: alunite (2), natroalunite (3) and lH$_3$O–alunite (4), (5) and (6) correspond to alunite and hydronium alunite respectively from Lager et al. 2001)

alunite powder at 600 °C over 12 h. The thermogravimetric analysis (TGA) and differential thermal analysis (DTA) were performed with a coupled thermal analyser (SETARAM TG/DTA 92) DTA-TGA instrument.

Measurements were taken from 25 to 1,200 °C at ambient atmosphere with a heating rate of 10 °C/min.

The powder diffraction measurement of alunite was conducted with the X'Pert MPD Pro PANalytical

Fig. 5 X-ray diffraction patterns in the 5°–100°, 2θ range of the compact alunite sample from El Gnater
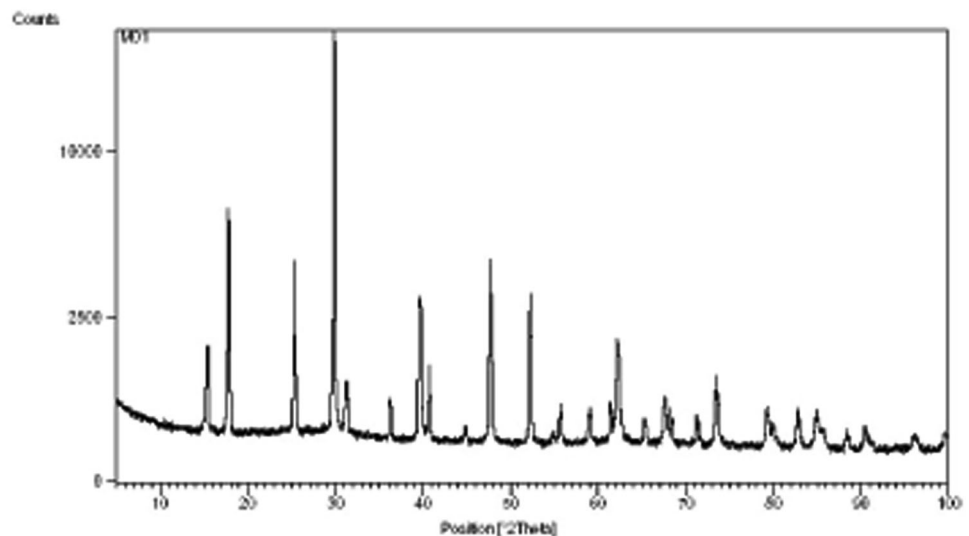
automated X-ray diffractometer at INRST using CuKa radiation.

The diffractograms were obtained over the 20th range from 3° to 100° at a scan speed of 1/2 deg/min.

Micromorphological investigation and qualitative elemental composition of various minerals in the samples were determined with a Philips XL30 scanning electron microscope (SEM) at the Sciences Faculty of Sfax: "Faculté des Sciences de Sfax (FSS)". The operating conditions are respectively maintained at 20 kV and 60 mA for the accelerating voltage and current intensity. The SEM specimens were prepared from freshly broken surfaces of the rocks. The powder was mounted on an Al metal stub, then covered with gold using a BAL122 TEC MED 020 coating system equipped with an argon gas for purging purposes. The microscope working distances ranged between 10 and 15 mm, with magnification up to 100,000×, depending on the height and quality of the crystals as well as on the efficiency of the gold coating. SEM micrographs of the solids were recorded with video-printer attached to the scanning electron microscope.

Geographic and geological setting

The alunite occurrence of Central Tunisia is located at El Gnater site (Kairouan District) at mid way between the cities of El Ala and Hajeb El Aioun (Fig. 1). From El Ala centre, a paved rural road leads towards the most outcrops of the El Gnater site. The latter corresponds to the periclinal closure of the Rebeiba anticline (Fig. 2). The heart of this tectonic structure is mainly Cenomano-Turonian marl overlaid by the middle and upper Eocene clay

sediments of the Cherahil formation. The El Gnater outcrop section shows three members (Fig. 3a).

The lower member (35 m thick) is mainly made up of bioclastic and dolomitic limestone. It begins with conglomeratic deposit that overlies Turonian marl of the Rbeiba structure;

- The middle member is made up of 120 m of alternations of sand, claystone and shelly limestone levels;
- The upper member (60 m thick) is dominated by clay deposit; it shows thin intercalations of shell and shelly oysters' rich limestone. This member is overlaid by Oligocene white sand.

Alunite occurs in three horizons of lenticular inter bedding at the top of the upper member (Fig. 3b), especially on the northern flank of the anticline structure. These horizons extend for at least 100 m and vary in thickness from 0.1 to 0.5 m (Fig. 4a). They are intercalated by thick sequences of green clay (2.2 m to about 7 m) and they contain secondary gypsum and thin veins of jarosite (Fig. 4b, c).

Results

Chemical composition

Chemical composition (Table 1) shows that El Gnater alunite is relatively pure member.

Only trace amounts of SiO_2 and Fe_2O_3 are detected. The former may correspond to a minor amount of clay minerals and the latter may be related to the presence of free iron oxide. However, some excessive water is observed, ($H_2O = 17.80$ %) compared to the chemical
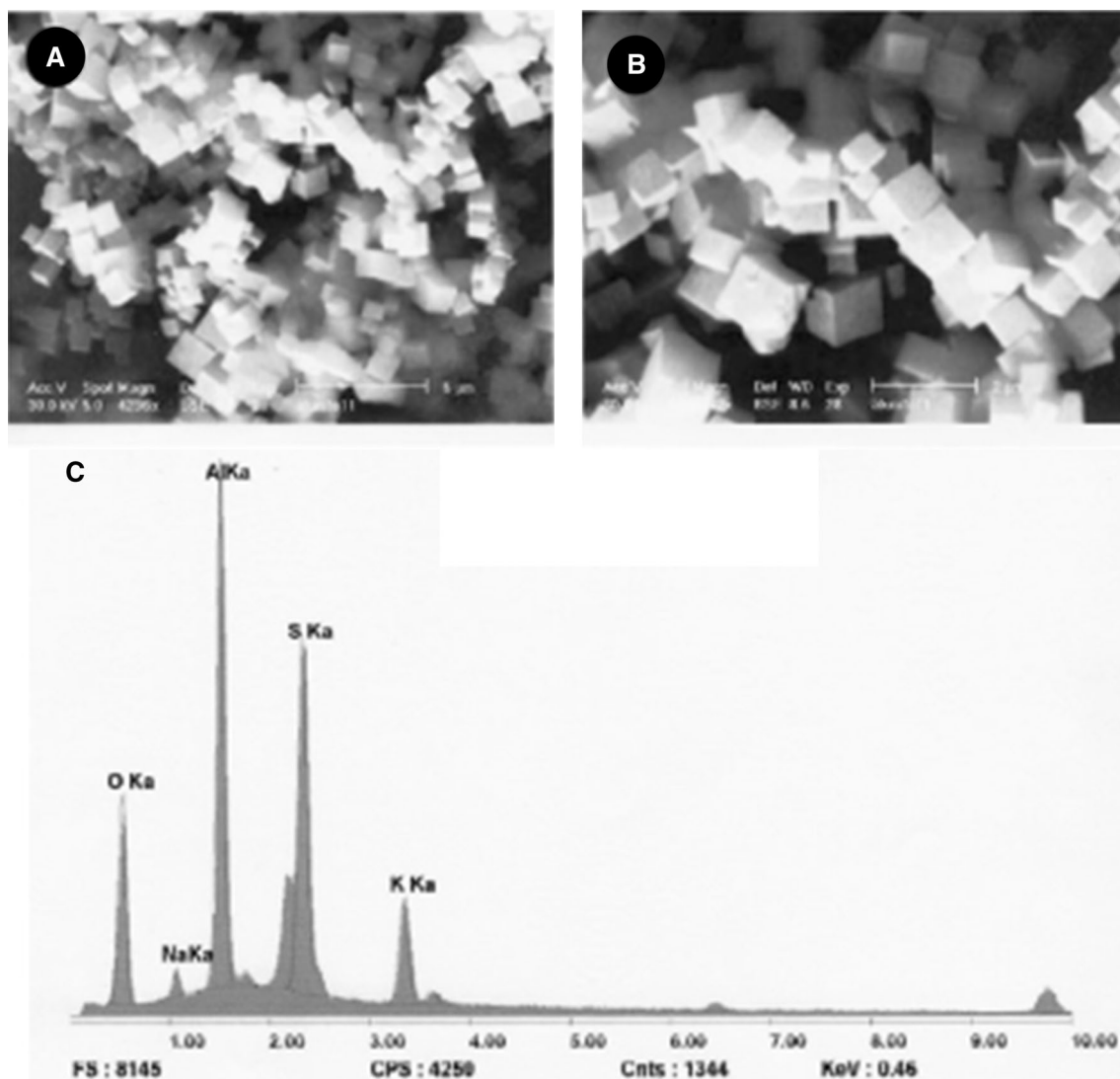
Fig. 6 SEM study of alunite sample: **a**, **b** SEM photomicrographs illustrating two different scales of pseudocubic small crystals of alunite; **c** qualitative microanalysis of single crystal of alunite

composition of an ideal alunite ($H_2O = 13\,\%$) and to the natural alunite (sample No. 5, Table 1). The deficiency of Al requires some excessive water and confirms the non-stoichiometry of the alunite (Hartig et al. 1984; Bohmhammel et al. 1987; Ripmeester et al. 1986; Lager et al. 2001).

El Gnater alunite structural formula is calculated on atomic value. Atomic number of SO_4 is fixed at 2 because percentage of this oxide is very similar from ideal alunite and the other cations are reported by correction: $(K_{0.89} Na_{0.27})\,Al_{2.76}(SO_4)_2(OH)_6$.

The amount of K_2O and Na_2O (11.31 wt%) is approximately equal to the expected amount of alkalis cations in the theoretical alunite (11.40 wt%). Hence, the alunite of El Gnater belongs to the alunite-natroalunite solid solution and is near end member.

Mineralogical characterisation

The mineralogy of the host clays has been identified by X-ray diffraction. Bulk rock contains quartz, gypsum, jarosite, feldspars and carbonates. The clay fraction is composed of 80 % smectite, 10 % kaolinite and 10 % illite (Gaied 1996).

The X-ray powder diffraction data of alunite (Fig. 5) confirm the chemical analysis and suggest the high purity of this substance according to the A.S.T.M files (14/130) and to Brown and Brindley (1980) data. The main diagnostic reflections of alunite occur approximately at 5.70, 4.93, 3.49, 2.97, 2.84, 2.26, 1.89, 1.74 and 1.641 Å (Fig. 5). These quite values prove notable agreement with alunite literature (Stoffregen and Alpers 1992; Lager et al. 2001; Rudolf et al. 2003).

Fig. 7 DTA and TGA curves of El Gnater alunite; loss of water = 17.27 % and loss of SO_3 = 29.09 %
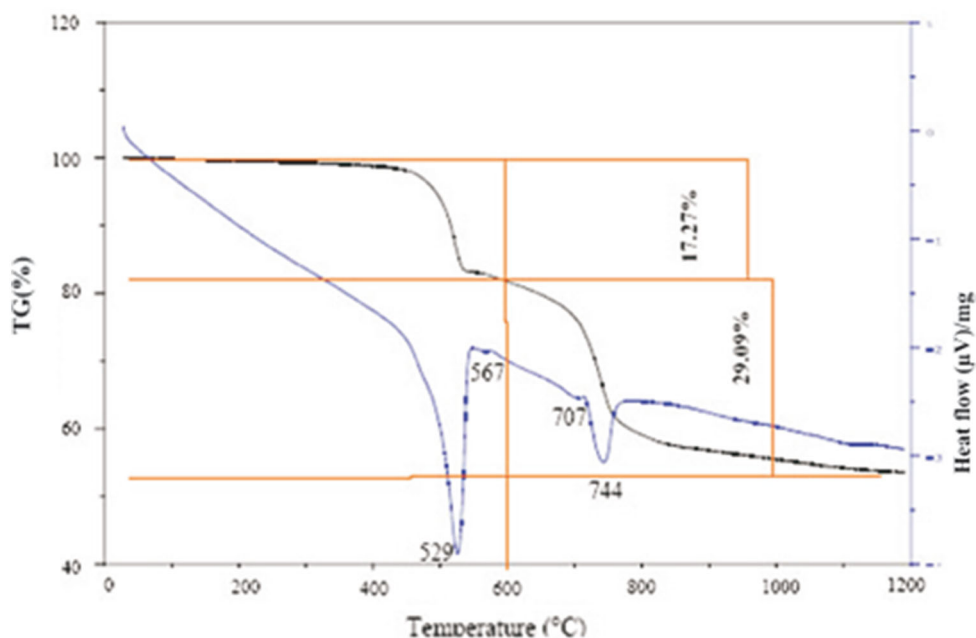
Scanning electronic microscope study

The SEM photographs show small well-formed pseudocubic crystals of alunite that are equigranular in diameter of approximately 1 μm in size (Fig. 6a, b). Qualitative microanalyses (Fig. 6c) indicate that S, Al, K, Na and oxygen are the major elements as expected from chemical composition of El Gnater alunite (Table 1).

Thermal analysis

Thermal analysis of alunite shows two well-defined stages of endothermic reactions corresponding respectively to dehydroxylation (loss of OH) and desulphuration (loss of SO_3) (Fig. 7) (Davey et al. 1963; Kubisz 1970; Slansky 1973; Fielding 1981; Pysiak and Glinka 1981; Bohmhammel et al. 1987). During the first endothermic reaction, at 520 °C, alunite is transformed to $KAl(SO_4)_2$ crystalline alkaline aluminium sulphate and to amorphous Al_2O_3. Whereas, during the second endothermic reaction, at 745 °C, the alkali aluminium sulphate is decomposed into aluminium oxide, alkali sulphate (K_2SO_4) with the loss of SO_2 (Bohmhammel et al. 1987; Piga 1995; Cipriani et al. 1997; Lager et al. 2001). These reactions and decomposition temperatures are explained by Piga (1995).

According to the TGA data, ignition loss at 600 °C (17.27 wt%) is higher than expected for alunite (13 wt%). Therefore, this loss should be expressed as structural bound OH and the non-OH structural bound H_2O. The latter (4.27 wt% excess) corresponds to the absorbed water as H_2O, H_3O^+ or some trace amounts of amorphous materials associated with the alunite separates. The excess of water (4.27 wt%) can be related to the H_2O and not to H_3O^+, because hydronium is not justified for this alunite.

Discussion

Generally alunite and jarosite formed in sedimentary environments are associated with clayey or terrigenous host sediments. This group of minerals may be authigenic interbedded with evaporitic ones, or hypogene product under hydrothermal alteration, or supergene product under anoxic conditions in open lagoon or intertidal zone. The latter can be likely the case for alunite studied. This alunitic mineralization was observed only at the top of the argillaceous formation of Late Eocene age, completing a regressive sequence. The presence of the jarosite, disseminated within the argillaceous levels, reflects oxidizing conditions. Whereas, alunite can be formed only under reducing conditions starting from the marine water supersaturated in cations Al^{3+}, K^+, Na^+ and in anion SO_4^{2-}. The cations are the products of alteration of smectitic clays of Late Eocene age. The excess of SO_4^{2-} can be linked to Ca^{2+} which can be released from calcic smectites to give laminated primary gypsum. The SO_4^{2-} was generated by sulphuric acid at warm temperature (about 30 °C) which may be attested by fine pseudocubic crystals of alunite that have about 1 μm as announced by Rye et al. (1992).

The El Gnater alunite has certainly diagenetic origin, but in which stage of diagenesis was it formed? Once compared with those met in Middle East which were formed in
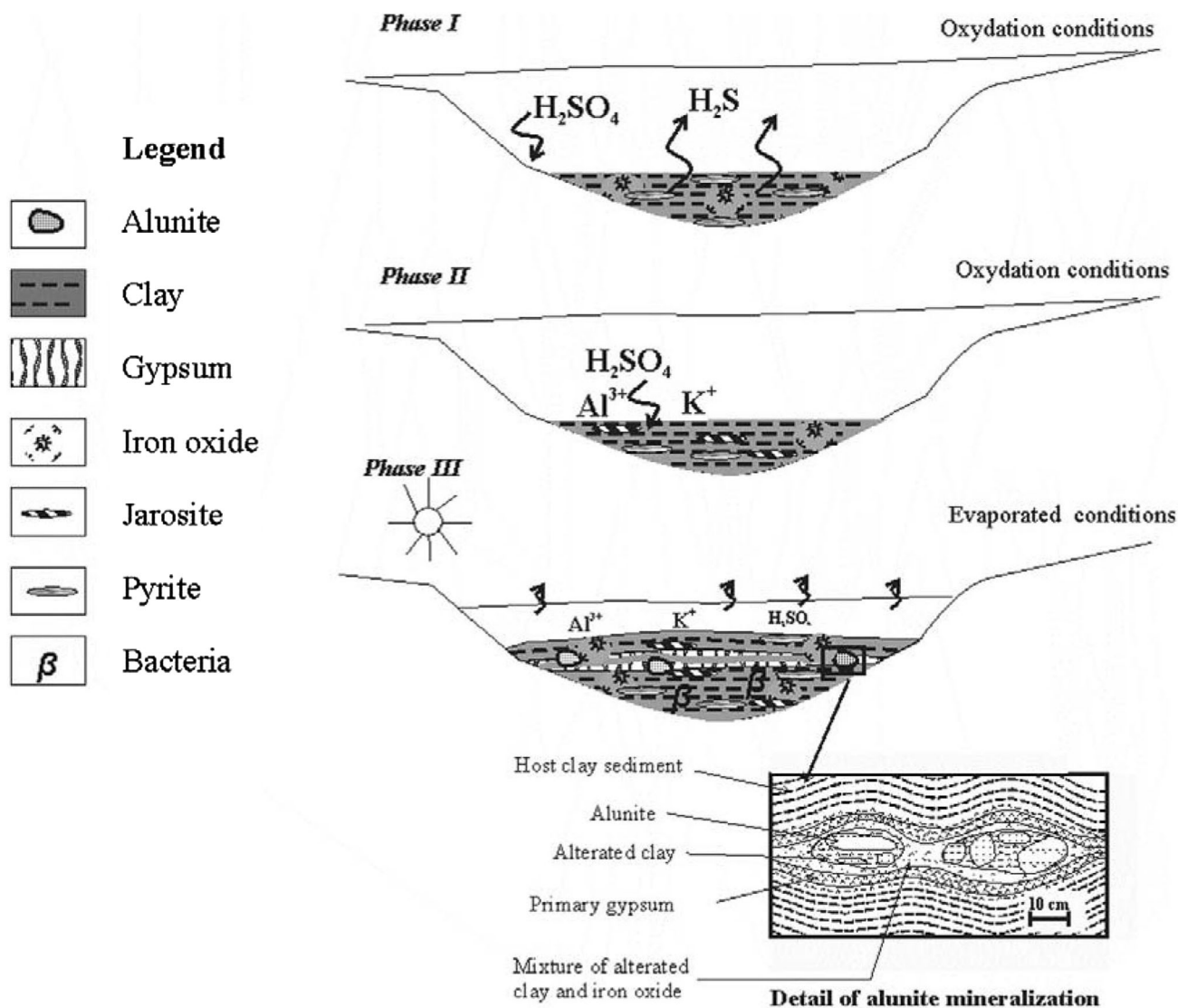
Fig. 8 Proposed genetic mode of alunite and associated minerals (jarosite, gypsum and hematite, etc....)

middle Miocene sedimentary environments, it can be affirmed that El Gnater occurrence is similar to Ras Sudar (Sinai, Egypt). It may be formed in late diagenesis conditions within a regressive sedimentary sequence represented by infra-tidal Eocene clay deposit grading to subtidal Oligocene sand deposit. This is indicated by the following:

- The interbedded of nodules horizons with the clay levels (Fig. 4a);
- The presence of syndiagenetic fault sealed by Fortuna sand deposit (Fig. 4a);
- The covering of the nodules by laminated primary gypsum (Fig. 4c).

Therefore, the preliminary approach of the El Gnater alunite genesis mode can be the following one (Fig. 8):

- *Phase I* Formation of sulphuric acid that results from tow oxidation reactions of the pyrite contained in clays deposit:

  1. $Fe_2S + 3H_2O \rightarrow Fe_2O_3 + H_2S$
  2. $H_2S + 2O_2 \rightarrow H_2SO_4$

- *Phase II* Formation of the jarosite by the following reaction: $K + Fe_2S + H_2O \rightarrow KFe_3(SO_4)_2(OH)_6$.
- *Phase III* Attack clays sediments rich in Al^{3+}, Na^+ and K^+ with H_2SO_4. The result is the formation of alunite: $(K_{0.89} Na_{0.27}) Al_{2.76}(SO_4)_2 (OH)_6$ and gypsum: $CaSO_4, 2H_2O$ in evaporated conditions.

In this phase, smectite clay minerals of the Late Eocene, rich with aluminium, potassium, calcium and sodium

change progressively to alunite under the action of the sulphuric acid.

This acid is probably due to the oxidization of sulphurized gas (H_2S) that comes from depths (Khalaf 1990) and/or from the oxidization of pyrite, which occurs frequently in the clay series. The presence of the iron oxide associated with the alunite pleads in favour of this last hypothesis. The stratification of El Gnater alunite with jarosite rich clay levels might be attributed to the lowering climatic conditions (Long et al. 1992). The oxidation conditions encourage more the jarosite crystallization than alunite which may explain the abundance disseminated jarosite more than alunite in the El Gnater region.

Conclusion

El Gnater alunite would probably crystallize in a sedimentary environment approximately at the top of the regressive deposit sequence between the Eocene tidal clays and the Oligocene subtidal sands. The white deposits of alunite occur as small lens and it was probably resulted from the sulphuric acid attack on smectitic clays during late diagenetic conditions. Chemical composition, X-ray powder diffraction, thermal analysis and SEM show that El Gnater alunite has characteristics close to the alunite end member. Its composition belongs to the K–Na alunite series.

It contains a slight excess of water and little amount of Na. The water excess can be related to the lack of Al and can be expressed by the adsorbed water molecule. The El Gnater alunite is very well crystallized as shown by SEM and the equigranular pseudocubic crystals are sized approximately 1 μm. Structural formula ($K_{0.93}$ $Na_{0.09}$) ($Al_{2.3}$ $S_{1.34}$) O_8 indicates the high purity of El Gnater alunite when compared with the published ones. Thermal analysis of El Gnater alunite is similar to the previously published data of pure alunite. The only dehydroxylation phase, identified here, indicates that the small excess of water reported from the chemical analysis is not related to the hydronium H_3O^+ and may be due to the loss of absorbed water H_2O.

The jarosite, which is the isostructural with the alunite, has been found in the same occurrence. But it is not organized in nodules like alunite and it is associated with secondary gypsum. The genesis of alunite can be attributed to the reducing climatic conditions. However, the oxidation conditions encourage the crystallization of jarosite. That is why there are more interbedded levels of jarosite than alunite.

References

Bohmhammel K, Naumann R, Paulik F (1987) Thermoanalytical and calorimetric investigations on the formation and decomposition of some alunites. Thermochim Acta 121:109–119

Brown G, Brindley GW (1980) Crystal structures of clay minerals and their X-ray identification. Mineralogical Society, London, pp 361–410

Chitale DV, Güven N (1987) Natroalunite in laterite profile over deccan trap basalts at Matanomadh, Kuth, India. Clays Clays Miner 35(3):196–202

Cipriani P, Marruzzo G, Piga L, Pochetti F (1997) Thermal behaviour of mixtures of an alunite ore with K_2CO_3, $CaCO_3$ and Ca (OH_2). Thermochim Acta 294:139–146

Davey PT, Lukaszewski GM, Scott TR (1963) Thermal decomposition of basic aluminium sulfate, $3Al_2O_3 \cdot 4SO_3 \cdot 9H_2O$. Aust J Appl Sci 14:137–154

Drouet C, Navrotsky A (2003) Synthesis, characterization and thermochemistry of K–Na–H_3O jarosites. Geochim Cosmochim Acta 67:2063–2076

Drouet C, Pass KL, Draucker S, Navrotsky A (2004) Thermochemistry of jarosite-alunite and natrojarosite–natroalunite solid solutions. Geochim Cosmochim Acta 68:2197–2205

Dutrizac JE, Jambor JL (2000) Jarosites and their application in hydrometallurgy. In: Ribbe PH (ed) Reviews in mineralogy and geochemistry: sulfate minerals, vol 40. Mineralogical Society of America, Washington, pp 405–452

Fielding SJ (1981) Crystal chemistry of the oxonium alunite–potassium alunite series. M.S. Thesis, Lehigh Univ., Bethlehem, Pennsylvania

Gaied ME (1991) Géologie des matériaux utiles de la région d'El Gnater (Tunisie centrale). Mémoire de DEA, Fac. Sci. Tunis, p 91

Gaied ME (1996) Etude géologique et géotechnique des matériaux utiles éocènes de la bordure nord-orientale du paléorelief de Kasserine (Tunisie centrale). Thèse de Doc. Spé. Fac. Sci. Tunis, p 203

Goldbery R (1980) Early diagenetic Na–alunites in Miocene algal mat intertidal facies, Ras Sudar, Sinai. Sedimentology 27:189–198

Hall RB (1978) World non-bauxite aluminium resources: alunite. Prof. Pag. U.S. Geol. Surv. 1076-A

Hartig C, Brand P, Bohmhammel K (1984) Fe–Al isomorphie undstrukturwasser in Kristallen von jarosit-alunit-Typ. Z Anorg Allg Chem 508:159–164

Keller WD, Gentile Richard J, Raesman AL (1967) Allophane and Na-rich alunite from kaolinite nodules in shale. J Sediment Petrol 37:215–220

Khalaf FJ (1990) Diagenetic alunite in clastic sequences, Kuwait, Arabian Gulf. Sedimentology 37:155–164

Kubisz J (1970) Studies on synthetic alkali–hydronium jarosites. I: synthesis of jarosite and natrojarosite. Mineral Pol I:47–59

Lager GA, Swayze GA, Loong CK, Rotella FJ, Richardson JW, Stoffregen RE (2001) Neutron spectroscopic study of synthetic alunite and oxonium substituted alunite. Can Miner 39:1131–1138

Lombardi K, Sheppard SMF (1977) Petrographic and isotopic studies of altered acid volcanics of the Tofa-Cerite area, Italy: the genesis of the clays. Clay Miner 12:47–161

Long DT, Fegan NE, Mckee JO, Lyons WB, Hines ME, Macumber PG (1992) Formation of alunite, jarosite and hydrous iron oxides in a hypersaline system: lake Tynell, Victoria, Australia. Chem Geol 96:183–203

Mutlu H, Sariiz K, Kadir S (2005) Geochemistry and origin of the Saphane alunite deposit, Western Anatolia, Turkey. Ore Geol Rev 26:39–50

Ossaka J, Hirabayashi JI, Okada K, Kobayashi R, Hayashi T (1982) Crystal structure of minamiite, a new mineral of the alunite group. Am Miner 67:114–119

Palmer AN, Palmer MV (1992) Geochemical and petrologic observations in Lechuguilla cave, New Mexico. In: Ogden AE (ed) Abstracts of the 1992 Friend of Karst. Cookeville, p 25–26

Piga L (1995) Thermogravimetry of a kaolinite–alunite ore. Thermochim Acta 265:177–187

Pysiak J, Glinka A (1981) Thermal decomposition of basic aluminium potassium sulfate. Part I: stages of decomposition. Thermochim Acta 44:21–28

Rattray KJ, Taylor MR, Bevan DJM, Pring A (1996) Compositional segregation and solid solution in the lead dominant alunite type minerals from Broken Hill, N. S. W. Miner Mag 60:779–785

Ripmeester JA, Ratcliffe CI, Dutrizac JE, Jambor JL (1986) Hydronium in the alunite jarosite group. Can Miner 22:773–784

Ross C, Bergquist R, Monroe WH, Fahey JJ, Ross M (1968) Natroalunite in upper cretaceous sedimentary rocks North-Central Texas. J Sediment Res 38(4):1155–1165

Rouchy JM, Pierre C (1987) Authigenic natroalunite in middle Miocene evaporates from the Gulf of Suez (Gemsa, Egypt). Sedimentology 34:807–812

Rudolf WW, Mason R, Schmidt P (2003) Synthetic alunites of the potassium–oxonium solid solution series and some other members of the group: synthesis, thermal and X-ray characterization. Eur J Miner 15:913–924

Rye RO, Bethka PM, Wasserman MD (1992) The stable isotope geochemistry of acid sulphate alteration. Econ Geol 87:225–262

Scott KM (1987) Solid solution in, and classification of, gossan-derived members of the alunite—jarosite family, northwest Queensland, Australia. Am Miner 72:178–187

Scott KM (2000) Nomenclature of the alunite supergroup: discussion. Can Miner 38:1295–1297

Slansky E (1973) The thermal investigation of alunite and natroalunite. N Jb Miner Mh 3:124–138

Stoffregen RE, Alpers CN (1992) Observations on the unit cell dimensions, H_2O content, and δD values of natural and synthetic alunite. Am Miner 77:1092–1098

Stoffregen RE, Alpers CN, Jambor JL (2000) Alunite–jarosite crystallography, thermodynamics, and geochemistry. In: Ribbe PH (ed) Reviews in mineralogy and geochemistry: sulphate minerals, vol 40. Mineralogical Society of America, Washington, pp 454–479